J|A|C|S ARTICLES

Published on Web 09/30/2009

Effects of Terminal Functional Groups on the Stability of the Polyproline II Structure: A Combined Experimental and Theoretical Study

Michael Kuemin,[†] Sabine Schweizer,[‡] Christian Ochsenfeld,*[,‡] and Helma Wennemers*[,†]

Department of Chemistry, University of Basel, St. Johanns-Ring 19, CH-4056 Basel, Switzerland, and Institute for Physical and Theoretical Chemistry, University of Tübingen, Auf der Morgenstelle 8, D-72076 Tübingen, Germany

Received July 31, 2009; E-mail: helma.wennemers@unibas.ch; christian.ochsenfeld@uni-tuebingen.de

Abstract: The conformational stability of the polyproline II (PPII) helix with respect to the functional groups at the C- and N-termini was examined both experimentally and theoretically. Oligoprolines AcN−$[Pro]_{12}$−$CONH_2$ (**1**), HN−$[Pro]_{12}$−$CONH_2$ (**2**), AcN−$[Pro]_{12}$−CO_2H (**3**), and HN−$[Pro]_{12}$−CO_2H (**4**) with charged and capped termini served as model compounds, and the relative ease with which they switch from the PPII to the polyproline I (PPI) helix was used as a measure to analyze their conformational stabilities. CD spectroscopic studies demonstrate that a positively charged N-terminus and a negatively charged C-terminus destabilize the PPII helix and favor the PPI helix, whereas capped termini favor the PPII over the PPI helix. These experimental findings are supported by the energy differences between the PPII and PPI helices of oligoprolines **1**−**4** computed by ab initio methods including electron-correlation effects (second-order Møller−Plesset perturbation theory, MP2). Furthermore, these quantum-chemical calculations show that differences in charge−dipole interactions are responsible for the experimentally and computationally observed relative stabilities. Although these electrostatic interactions between the terminal charges and the amide dipoles stabilize both helices, they are significantly stronger in the PPI helix where the amide bonds are oriented almost linear to the helix axis as compared to the PPII helix in which the amides are nearly perpendicular to the axis. Moreover, we demonstrate that a negative charge at the C-terminus has a more pronounced effect on the relative stability as compared to a positive charge at the N-terminus due to destabilization of the PPII helix by repulsive interaction between the C-terminal carboxylate with the neighboring amide bond. Studies at different pH values verified the electrostatic nature of the observed effects and demonstrate how changes in the protonation state can be used to deliberately stabilize the PPII helix over the PPI helix or vice versa.

Introduction

The polyproline II (PPII) helix is widespread in nature and plays important roles in many biological processes such as signal transduction, transcription, immune response, and cell motility.[1] In addition, the single strands of collagen with the typical $[Pro-Hyp-Gly]_n$ repeat unit adopt a PPII-like conformation.[2] The PPII helix has also been proposed as an important local conformation in disordered states of proteins that are relevant for protein folding.[3,4] Furthermore, oligoprolines have been used as molecular spacers for studying, for example, energy or electron transport[5,6] and are attractive as functionalizable molecular scaffolds that allow for switching between the PPII and the more compact PPI helix.[7] Understanding factors that influence the PPII conformation is therefore an important goal.

[†] University of Basel.

[‡] University of Tübingen.

(1) For reviews, see: (a) Rath, A.; Davidson, A. R.; Deber, C. M. *Biopolymers (Pept. Sci.)* **2005**, *80*, 179–185. (b) Cubellis, M. V.; Caillez, F.; Blundell, T. L.; Lovell, S. C. *Proteins* **2005**, *58*, 880–892. (c) Bochicchio, B.; Tamburro, A. M. *Chirality* **2002**, *14*, 782–792. (d) Holt, M. R.; Koffer, A. *Trends Cell Biol.* **2001**, *11*, 38–46. (e) Kay, B. K.; Williamson, M. P.; Sudol, M. *FASEB J.* **2000**, *14*, 231–241. (f) Stapley, B. J.; Creamer, T. P. *Protein Sci.* **1999**, *8*, 587–595. (g) Silifardi, G.; Drake, A. F. *Biopolymers* **1995**, *37*, 281–92.

(2) For recent reviews, see: (a) Shoulders, M. D.; Raines, R. T. *Annu. Rev. Biochem.* **2009**, *78*, 929–958. (b) Brodsky, B.; Thiagarajan, G.; Madhan, B.; Kar, K. *Biopolymers* **2008**, *89*, 345–353. (c) Engel, J.; Bächinger, H. P. *Top. Curr. Chem.* **2005**, *247*, 7–33.

(3) For reviews, see: (a) Shi, Z.; Chen, K.; Liu, Z.; Kallenbach, N. R. *Chem. Rev.* **2006**, *106*, 1877–1897. (b) Woody, R. W. *Adv. Biophys. Chem.* **1992**, *2*, 37–79.

(4) (a) Dukor, R. K.; Keiderling, T. A. *Biopolymers* **1991**, *31*, 1747–1761. (b) Krimm, S.; Tiffany, M. L. *Isr. J. Chem.* **1974**, *12*, 189–200.

(5) (a) Doose, S.; Neuweiler, H.; Barsch, H.; Sauer, M. *Proc. Natl. Acad. Sci. U.S.A.* **2007**, *104*, 17400–17405. (b) Schuler, B.; Lipman, E. A.; Steinbach, P. J.; Klumke, M.; Eaton, W. A. *Proc. Natl. Acad. Sci. U.S.A.* **2005**, *102*, 2754–2759. (c) Stryer, L.; Haugland, R. P. *Proc. Natl. Acad. Sci. U.S.A.* **1967**, *58*, 719–726.

(6) (a) Cordes, M.; Kottgen, A.; Jasper, C.; Jacques, O.; Boudebous, H.; Giese, B. *Angew. Chem., Int. Ed.* **2008**, *47*, 3461–3463. (b) Serron, S. A.; Iii, A. W. S.; Fleming, C. N.; Danell, R. M.; Baik, M.-H.; Sykora, M.; Dattelbaum, D. M.; Meyer, T. J. *J. Am. Chem. Soc.* **2004**, *126*, 14506–14514.

(7) (a) Erdmann, R. S.; Kuemin, M.; Wennemers, H. *Chimia* **2009**, *63*, 197–200. (b) Kümin, M.; Sonntag, L.-S.; Wennemers, H. *J. Am. Chem. Soc.* **2007**, *129*, 466–467.

 10.1021/ja906466q CCC: $40.75

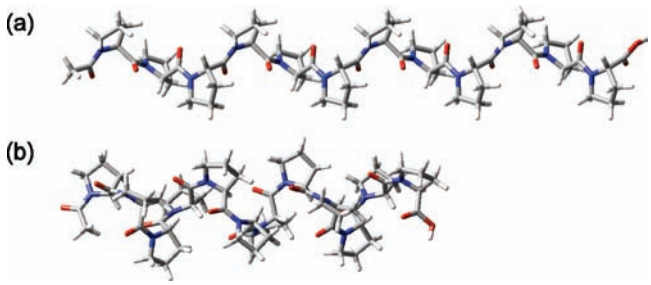

Figure 1. Models of the (a) PPII and (b) PPI conformation of AcN−$[Pro]_{12}$−CO_2H.

An ideal PPII helix has dihedral angles ϕ and ψ of −75° and +145°, respectively, and all amide bonds are in trans conformations ($\omega = 180°$), resulting in a left-handed helix with every third residue stacked on top of each other in a lateral distance of 9.4 Å (Figure 1a).[8,9] Within the PPII helix, all amide bonds of the peptide backbone are nearly perpendicular to the helix axis. Many studies directed toward an understanding of the PPII helix stability utilized oligoprolines as model systems because they adopt the PPII conformation in water already at short chain lengths.[9−15] Several studies also took advantage of the ability of oligoprolines to adopt a distinctly different helical structure, the polyproline I (PPI) conformation, which occurs in more hydrophobic environments such as aliphatic alcohols.[7,9−11] The PPI helix is in contrast to the PPII helix right-handed, and all amide bonds are in cis conformations ($\omega = 0°$) with ϕ and ψ angles of −75° and +160°, respectively.[9,16] These dihedral angles result in a more compact structure (helical pitch of 5.6 Å per turn, 3.3 proline residues per turn) with the amide bonds oriented nearly parallel to the PPI helix axis (Figure 1b). In contrast to the α-helix, neither the PPII nor the PPI helix is stabilized by intramolecular hydrogen bonds.

With the help of oligoproline model systems, Creamer and co-workers established a propensity scale for amino acids to adopt the PPII helix by incorporating different amino acid residues into oligoprolines and comparing the conformational stability of these "host−guest systems".[12] Interactions between side-chain functional groups and the effect of solvation by water−backbone interactions have been examined by several researchers as determinants of the PPII conformational stability.[13−15] For collagen, Raines and co-workers and several other groups showed that interactions between the backbone amides have a stabilizing effect.[2a,17−19] We have recently shown that such stereoelectronic interactions are also crucial for the stability of oligoprolines.[7,20] Aside from these experimental studies, calculations have been performed to examine the conformational behavior of oligoprolines (for a brief discussion, see the Supporting Information).[21,22] At the ab initio level, mainly systems with comparatively small sizes have been studied.[21,22]

Little is known about the influence of the functional groups at the C- and N-termini of the PPII helix on its conformational stability.[23,24] This is in contrast to studies on α-helical structures and certain β-peptides where the effect of capped and free termini on the conformational stability has been investigated.[25,26] Here, we present a detailed analysis of the influence of charged and neutral functional groups at the N- and C-termini of oligoprolines on the conformational stability of the PPII and the PPI helix by comparing the ease of the PPII/PPI isomer-

(8) Cowan, P. M.; McGavin, S. *Nature* **1955**, *176*, 501–503.
(9) Rabanal, F.; Ludevid, M. D.; Giralt, E. *Biopolymers* **1993**, *33*, 1019–1028.
(10) (a) Kakinoki, S.; Hirano, Y.; Oka, M. *Polym. Bull.* **2005**, *53*, 109–115. (b) Rothe, M.; Rott, H.; Mazanek, J. *Pept., Proc. Eur. Pept. Symp., 14th* **1976**, 309–318.
(11) (a) Zhang, A.; Guo, Y. *Chem.-Eur. J.* **2008**, *14*, 8939–8946. (b) Moretto, A.; Terrenzani, F.; Crisma, M.; Formaggio, F.; Kaptein, B.; Broxtermann, Q. B.; Toniolo, C. *Biopolymers* **2007**, *89*, 465–469. (c) Horng, J.-C.; Raines, R. T. *Protein Sci.* **2006**, *15*, 74–83. Mutter, M.; Wohr, T.; Gioria, S.; Keller, M. *Biopolymers* **1999**, *51*, 121–128. (d) Engel, J.; Schwarz, G. *Angew. Chem., Int. Ed. Engl.* **1970**, *9*, 389–400.
(12) (a) Chellgren, B. W.; Creamer, T. P. *Biochemistry* **2004**, *43*, 5864–5869. (b) Rucker, A. L.; Pager, C. T.; Campbell, M. N.; Qualls, J. E.; Creamer, T. P. *Proteins* **2003**, *53*, 68–75. (c) Kelly, M. A.; Chellgren, B. W.; Rucker, A. L.; Troutman, J. M.; Fried, M. G.; Miller, A.-F.; Creamer, T. P. *Biochemistry* **2001**, *40*, 14376–14383.
(13) Chellgren, B. W.; Creamer, T. P. *J. Am. Chem. Soc.* **2004**, *126*, 14734–14735.
(14) Whittington, S. J.; Creamer, T. P. *Biochemistry* **2003**, *42*, 14690–14695.
(15) (a) Mezei, M.; Fleming, P. J.; Srinivasan, R.; Rose, G. D. *Proteins* **2004**, *55*, 502–507. (b) Pappu, R. V.; Rose, G. D. *Protein Sci.* **2002**, *11*, 2437–2455. (c) Creamer, T. P.; Campbell, M. N. *Adv. Protein Chem.* **2002**, *62*, 263–282. (d) Schimmel, P. R.; Flory, P. J. *Proc. Natl. Acad. Sci. U.S.A.* **1967**, *58*, 52–59.
(16) Traub, W.; Shmueli, U. *Nature* **1963**, *198*, 1165–1166.
(17) (a) Hinderaker, M. P.; Raines, R. T. *Protein Sci.* **2003**, *12*, 1188–1194. (b) Bretscher, L. E.; Jenkins, C. L.; Taylor, K. M.; DeRider, M. L.; Raines, R. T. *J. Am. Chem. Soc.* **2001**, *123*, 777–778. (c) Holmgren, S. K.; Taylor, K. M.; Bretscher, L. E.; Raines, R. T. *Nature* **1998**, *392*, 666–667.
(18) (a) Cadamuro, S. A.; Reichold, R.; Kusebauch, U.; Musiol, H.-J.; Renner, C.; Tavan, P.; Moroder, L. *Angew. Chem., Int. Ed.* **2008**, *47*, 2143–2146. (b) Improta, R.; Berisio, R.; Vitagliano, L. *Protein Sci.* **2008**, *17*, 955–961. (c) Dai, N.; Wang, X. J.; Etzkorn, F. A. *J. Am. Chem. Soc.* **2008**, *130*, 5396–5397.
(19) For other examples of n → π^* interactions, see: (a) Choudhary, A.; Gandla, D.; Krow, G. R.; Raines, R. T. *J. Am. Chem. Soc.* **2009**, *131*, 7244–7246. (b) Shah, N. H.; Butterfoss, G. L.; Nguyen, K.; Yoo, B.; Bonneau, R.; Rabenstein, D. L.; Kirshenbaum, K. *J. Am. Chem. Soc.* **2008**, *130*, 16622–16632. (c) Gorske, B. C.; Bastian, B. L.; Geske, D. G.; Blackwell, H. L. *J. Am. Chem. Soc.* **2007**, *129*, 8928–8929. (d) Maccallum, P. H.; Poet, R.; Milner-White, E. J. *J. Mol. Biol.* **1995**, *248*, 374–384.
(20) Sonntag, L.-S.; Schweizer, S.; Ochsenfeld, C.; Wennemers, H. *J. Am. Chem. Soc.* **2006**, *128*, 14697–14703.
(21) (a) Bour, P.; Kubelka, J.; Keiderling, T. A. *Biopolymers* **2002**, *65*, 45–59. (b) Kang, Y. K.; Jhon, J. S.; Park, H. S. *J. Phys. Chem. B* **2006**, *110*, 17645–17655. (c) Zhong, H.; Carlson, H. A. *J. Chem. Theory Comput.* **2006**, *2*, 342–353. (d) Kapitan, J.; Baumruk, V.; Bour, P. *J. Am. Chem. Soc.* **2006**, *128*, 2438–2443. (e) Counterman, A. E.; Clemmer, D. E. *J. Phys. Chem. B* **2004**, *108*, 4885–4898. (f) Holzwarth, G.; Backman, K. *Biochemistry* **1969**, *8*, 883–887.
(22) (a) Vila, J. A.; Baldoni, H. A.; Ripoll, D. R.; Ghosh, A.; Scheraga, H. A. *Biophys. J.* **2004**, *86*, 731–742. (b) Tanaka, S.; Scheraga, H. A. *Macromolecules* **1974**, *7*, 698–705. (c) Tanaka, S.; Scheraga, H. A. *Macromolecules* **1975**, *8*, 504–516. (d) Tanaka, S.; Scheraga, H. A. *Macromolecules* **1975**, *8*, 516–521. (e) Tanaka, S.; Scheraga, H. A. *Macromolecules* **1975**, *8*, 623–631.
(23) For previously observed experimental differences between protected and unprotected N-termini of PPII helices, see ref 10b and: (a) Crespo, L.; Sanclimens, G.; Montaner, B.; Perez-Tomas, R.; Royo, M.; Pons, M.; Albericio, F.; Giralt, E. *J. Am. Chem. Soc.* **2002**, *124*, 8876–8883. (b) Zhang, R.; Madalengoitia, J. S. *Tetrahedron Lett.* **1996**, *37*, 6235–6238.
(24) For a review on the role of charges in proteins in general, see: Gitlin, I.; Carbeck, J. D.; Whitesides, G. M. *Angew. Chem., Int. Ed.* **2006**, *45*, 3022–3060.
(25) (a) Sengupta, D.; Behera, R. N.; Smith, J. C.; Ulmann, G. M. *Structure* **2005**, *13*, 849–855. (b) Fairman, R.; Shoemaker, K. R.; York, E. J.; Stewart, J. M.; Baldwin, R. L. *Proteins* **1989**, *5*, 1–7. (c) Shoemaker, K. R.; Kim, P. S.; York, E. J.; Stewart, J. M.; Baldwin, R. L. *Nature* **1987**, *326*, 563–567. (d) Shoemaker, K. R.; Kim, P. S.; Brems, D. N.; Marqusee, S.; York, E. J.; Chaiken, I. M.; Stewart, J. M.; Baldwin, R. L. *Proc. Natl. Acad. Sci. U.S.A.* **1985**, *82*, 2349–2353. (e) Hol, W. G. J. *Prog. Biophys. Mol. Biol.* **1985**, *45*, 149–195.
(26) (a) Gee, P. J.; van Gunsteren, W. F. *Proteins* **2006**, *63*, 136–143. (b) Hart, S. A.; Bahadoor, B. F.; Matthews, E. E.; Qiu, X. J.; Schepartz, A. *J. Am. Chem. Soc.* **2003**, *125*, 4022–4023. (c) Seebach, D.; Abele, S.; Gademann, K.; Guichard, G.; Hintermann, T.; Jaun, B.; Matthews, J. L.; Schreiber, J. V. *Helv. Chim. Acta* **1998**, *81*, 932–982.

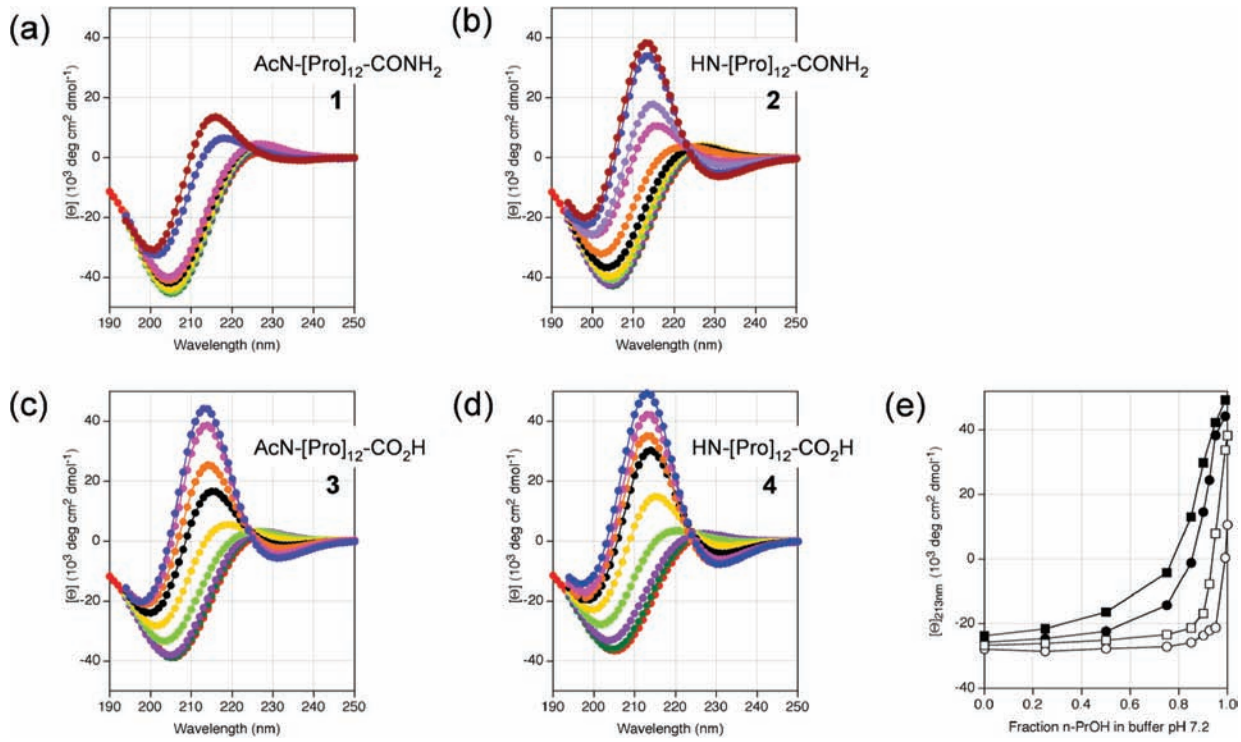

Figure 2. (a)−(d) CD spectra of **1** (a), **2** (b), **3** (c), and **4** (d) in mixtures of aqueous phosphate buffer (10 mM, pH 7.2) and *n*-PrOH. Phosphate buffer (red), 25% vol/vol *n*-PrOH in buffer (dark green), 50% *n*-PrOH (purple), 75% *n*-PrOH (light green), 85% *n*-PrOH (yellow), 90% *n*-PrOH (black), 92.5% *n*-PrOH (orange), 95% *n*-PrOH (pink), 99% *n*-PrOH (blue), and *n*-PrOH (brown). Spectra were recorded at concentrations of 50 μM (6×10^{-4} M per residue) at 25 °C. The solubility of peptides **3** and **4** did not allow for recording spectra in pure *n*-PrOH. For peptide **2** an additional spectrum was recorded in 97.5% *n*-PrOH (lavender). (e) CD signal at 213 nm for peptides **1** (○), **2** (□), **3** (●), and **4** (■) plotted against the fraction of *n*-PrOH in phosphate buffer (10 mM, pH 7.2).

ization for a series of model compounds. CD spectroscopic experiments demonstrate that charged terminal groups facilitate the conformational change from the PPII into the PPI helix. Furthermore, the experiments show that a negative charge at the C-terminus has a more pronounced effect as compared to a positive charge at the N-terminus due to a destabilization of the PPII helix. In addition, we present quantum-chemical calculations using linear-scaling methods[27,28] for oligoprolines up to the 15-mer, which provide results that are in agreement with the experimentally observed trends and allow for deeper insights into the specific intramolecular interactions.

Results and Discussion

Design of Model Compounds and Thermal Denaturation Studies. To study the effect of charged and charge-neutral functional groups at the N- and C-termini of a PPII helix, we prepared four oligoprolines consisting of 12 proline residues that differ in the functionalization at the C- and N-termini. Peptide AcN−$[Pro]_{12}$−$CONH_2$ (**1**) is neutral at both ends, peptide HN−$[Pro]_{12}$−$CONH_2$ (**2**) bears at pH 7 a positive charge at the N-terminus, peptide AcN−$[Pro]_{12}$−CO_2H (**3**) has a negative charge at the C-terminus, and peptide HN−$[Pro]_{12}$−CO_2H (**4**) possesses charges at either end at neutral pH (Scheme 1).[29]

Scheme 1. Oligoprolines **1**−**4** with Different Functional Groups at the C- and N-Termini[29]

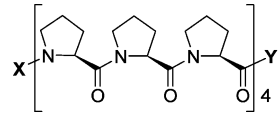

1: X = Ac; Y = NH_2; AcN-$[Pro]_{12}$-$CONH_2$
2: X = H; Y = NH_2; HN-$[Pro]_{12}$-$CONH_2$
3: X = Ac; Y = OH; AcN-$[Pro]_{12}$-CO_2H
4: X = H; Y = OH; HN-$[Pro]_{12}$-CO_2H

We started our investigations by recording CD spectra of all four model peptides in aqueous phosphate buffer pH 7.2 at a concentration of 50 μM. All spectra were similar, showing minima at 205 nm and maxima at 228 nm typical for the PPII helix.[9−11] We then heated the samples from 10 to 80 °C to study thermal denaturation. However, as expected from previous studies,[12b] only marginal changes in the CD spectra were seen, and clearly no thermal unfolding was observed (see the Supporting Information). This demonstrates the high thermal conformational stability of the PPII helix and showed that thermal denaturation does not allow for analyzing differences in the conformational stabilities of peptides **1**−**4**. We therefore evaluated the stability of the PPII conformation with respect to the functional groups at the termini by studying the ease with which oligopeptides **1**−**4** switch from the PPII to the PPI conformation.[7,11d]

Switching from the PPII to the PPI Helix. The PPII helix is the predominant conformation of oligoprolines in water, whereas the PPI helix is favored in solvents such as *n*-PrOH.[9−11] The amount of *n*-PrOH needed to switch the PPII helix to the PPI helix therefore reflects the ease of the conformational change between the PPII and the PPI form and can serve as a measure for their relative stabilities.[7,11d] To test the influence of the C- and N-terminal functional groups on the stability of the PPII helix, we studied the conformation of oligoprolines **1**−**4** in

(27) (a) White, C. A.; Johnson, B. G.; Gill, P. M. W.; Head-Gordon, M. *Chem. Phys. Lett.* **1994**, *230*, 8–16. (b) Shao, Y.; White, C. A.; Head-Gordon, M. *J. Chem. Phys.* **2001**, *114*, 6572–6577.
(28) (a) Ochsenfeld, C.; White, C. A.; Head-Gordon, M. *J. Chem. Phys.* **1998**, *109*, 1663–1669. (b) Ochsenfeld, C. *Chem. Phys. Lett.* **2000**, *327*, 216–223.
(29) To emphasize the terminal functional groups, we do not use the IUPAC abbreviation system for peptides but the denotation shown in Scheme 1.

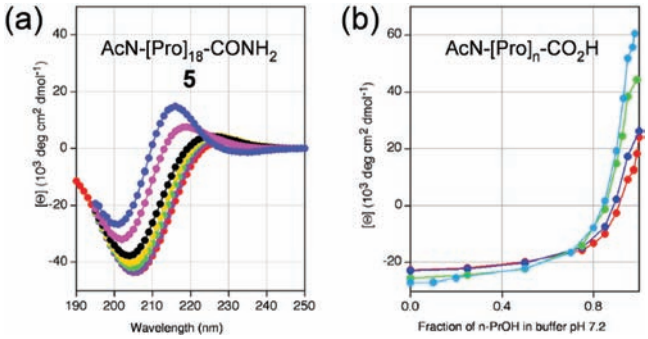

Figure 3. (a) CD spectra of AcN−[Pro]$_{18}$−CONH$_2$ (**5**) in mixtures of aqueous phosphate buffer (10 mM, pH 7.2) and *n*-PrOH. Phosphate buffer (red), 25% vol/vol *n*-PrOH in buffer (dark green), 50% *n*-PrOH (purple), 75% *n*-PrOH (light green), 85% *n*-PrOH (yellow), 90% *n*-PrOH (black), 95% *n*-PrOH (pink), and 98% *n*-PrOH (blue). Spectra were recorded at concentrations of 6×10^{-4} M per residue at 25 °C. (b) CD signal at 213 nm for peptides AcN−[Pro]$_n$−CO$_2$H plotted against the fraction of *n*-PrOH in phosphate buffer (10 mM, pH 7.2) with $n = 6$ (red, **3a**), $n = 9$ (blue, **3b**), $n = 12$ (green, **3**), and $n = 18$ (light blue, **3c**).

different mixtures of aqueous phosphate buffer (10 mM, pH 7.2) and *n*-PrOH by CD spectroscopy (Figure 2). These studies revealed remarkable differences between the four model compounds: peptide **4**, bearing charges at both the N- and the C-terminus, switches readily from the PPII to the PPI conformation. The CD spectrum of **4** in, for example, 95 vol % *n*-PrOH in buffer is typical for a PPI helix with a maximum at 213 nm and minima at 199 and 230 nm (Figure 2d, pink). In contrast, peptide **1** with capped termini adopts under the same conditions (95 vol % *n*-PrOH in buffer) still the PPII helix (Figure 2a, pink). Only in pure *n*-PrOH is the CD spectrum of **1** resembling that of a PPI helix (Figure 2a, brown). Thus, capped termini stabilize the PPII helix, whereas charges have a destabilizing effect.

A comparison of the CD spectra of peptides **2** and **3** shows that a negative charge at the C-terminus has a more pronounced destabilizing effect as compared to a positive charge at the N-terminus. Whereas 95 vol % *n*-PrOH is necessary to switch peptide **2** with an ammonium group at the N-terminus from the PPII to the PPI conformation (Figure 2b, pink), 85 vol % *n*-PrOH suffices to initiate this switch in the conformation of peptide **3** with a carboxylate at the C-terminus to a similar extent (Figure 2c, yellow line). A plot of the fraction of *n*-PrOH against the intensity of the signal at 213 nm indicative of the PPI helix summarizes these results (Figure 2e). It illustrates that the amount of *n*-PrOH needed to switch from the PPII to the PPI helix increases from peptide **4** to **1**, corresponding to an increase in the stability of the PPII helix from **4** to **1**. These results demonstrate not only that charges at the termini destabilize the PPII helix but also that a negative charge at the C-terminus destabilizes the PPII helix to a significantly larger extent as compared to a positive charge at the N-terminus.

It is known that switching from the PPII to the PPI helix becomes more favored with longer chain lengths of the oligoprolines.[10] To obtain an estimate of whether the chain length or the charge at the termini has a more pronounced effect on the PPII/PPI equilibrium, we investigated analogues of peptides **1** and **3**. The analogue of **1** with 18 residues AcN−Pro$_{18}$−CONH$_2$ (**5**) has a slightly higher tendency to adopt a PPI helix than does the 12-mer AcN−[Pro]$_{12}$−CONH$_2$ (**1**). 95% *n*-PrOH instead of 99% *n*-PrOH suffices to initiate the switch (Figure 3a); however, a pure PPI conformation is never adopted by **5** either. A similar trend toward a slightly facilitated switch is observed for homologues of peptide **3**. Figure 3b shows for the homologues AcN−[Pro]$_n$−CO$_2$H with $n = 6$, 9, 12, 18 (**3a**, **3b**, **3**, and **3c**) the CD signal at 213 nm (maximum in the CD spectra of the PPI helix) in dependence of the solvent composition, which serves as in Figure 2e as a measure for the tendency of the oligoprolines to adopt a PPI conformation. Longer chain lengths favor the PPI helix, but the effects are smaller as compared to the influence of the terminal functional groups.

Ab Initio Studies of Energetics of PPII and PPI Helices. To investigate the experimentally observed trends of the relative stability for the PPII and PPI helices in more detail, we performed quantum-chemical calculations for the peptides AcN−[Pro]$_{12}$−CONH$_2$ (**1**), $^+$H$_2$N−[Pro]$_{12}$−CONH$_2$ (protonated **2**), AcN−[Pro]$_{12}$−CO$_2^-$ (deprotonated **3**), and $^+$H$_2$N−[Pro]$_{12}$−CO$_2^-$ (zwitterionic **4**). To avoid an overestimation of a hydrogen bond between the C-terminal amide and the carbonyl group of the preceding amide group,[30] we also studied AcN−[Pro]$_{12}$−CO$_2$CH$_3$ (**1′**) and $^+$H$_2$N−[Pro]$_{12}$−CO$_2$CH$_3$ (**2′**) in which the C-terminal amides are replaced by ester moieties as model systems for peptides **1** and **2**, respectively. Additionally, we studied oligoprolines with different chain lengths and analyzed the contribution of individual proline residues.

Initial structures were generated using the program package Maestro[31] with idealized torsion angles for the PPII and PPI backbones based on structural data derived from X-ray structural analyses.[8,16] This well-defined structure provided a useful starting point for our systematic computational study. The initial structures were optimized at the HF/6-31G** level,[32,33] and energetics were computed by single-point RI-MP2/SVP[34,35] calculations. The latter method was found to be a good compromise between accuracy and feasibility of the calculations. Details on the structures and the choice of methods are given in the Supporting Information.

In Table 1, the computed energy differences between the PPI and PPII helices obtained at the RI-MP2/SVP//HF/6-31G** level are compared for the four types of peptides with differently charged end groups and various chain lengths in the gas phase. It is important to note that the energetic preference is less reliable by applying HF or B3LYP approximations. The computed MP2 data predict for the gas phase that the PPI helix is generally favored over the PPII helix. Two trends are observed: (a) With increasing chain lengths, the PPI helix becomes energetically more and more favored regardless of the charge at the termini. From a theoretical point of view, we note in passing that for a description of this trend the HF level is not sufficient, but

(30) (a) Taylor, C. M.; Hardré, R.; Edwards, P. J. B.; Park, J. H. *Org. Lett.* **2003**, *5*, 4413–4416. (b) Liang, G. B.; Rito, C. J.; Gellman, S. H. *Biopolymers* **1992**, *32*, 293–301.
(31) *Maestro 7.5*; Schrödinger Inc.: Portland, OR, 2005.
(32) (a) Hartree, D. R. *Proc. Cambridge Philos. Soc.* **1928**, *24*, 89–110. (b) Hartree, D. R. *Rep. Prog. Phys.* **1947**, *11*, 113–143. (c) Fock, V. *Z. Phys. A* **1930**, *61*, 126–148. (d) Szabo, A.; Ostlund, N. S. *Modern Quantum Chemistry*; Dover Publications Inc.: Mineola, NY, 1989.
(33) (a) Hehre, W. J.; Ditchfield, R.; Pople, J. A. *J. Chem. Phys.* **1972**, *56*, 2257–2261. (b) Hariharan, P. C.; Pople, J. A. *Theor. Chim. Acta* **1973**, *28*, 213–222.
(34) (a) Dunlap, B. I.; Connolly, J. W. D.; Sabin, J. R. *J. Chem. Phys.* **1979**, *71*, 3396–3402. (b) Vahtras, O.; Almlöf, J.; Feyereisen, M. W. *Chem. Phys. Lett.* **1993**, *213*, 514–518. (c) Eichkorn, K.; Treutler, O.; Oehm, H.; Häser, M.; Ahlrichs, R. *Chem. Phys. Lett.* **1995**, *240*, 283–289. (d) Eichkorn, K.; Weigend, F.; Treutler, O.; Ahlrichs, R. *Theor. Chem. Acc.* **1997**, *97*, 119–124. (e) Weigend, F.; Häser, M. *Theor. Chem. Acc.* **1997**, *97*, 331–340.
(35) Schäfer, A.; Horn, H.; Ahlrichs, R. *J. Chem. Phys.* **1992**, *97*, 2571–2577.

Table 1. Energy Differences at the RI-MP2/SVP//HF/6-31G** Level in kJ mol^{-1} between the PPI and PPII ($\Delta E = E_{PPI} - E_{PPII}$) Conformation of AcN−[Pro]$_x$−CONH$_2$ (**1**), AcN−[Pro]$_x$−CO$_2$CH$_3$ (**1′**), $^+$H$_2$N−[Pro]$_x$−CONH$_2$ (**2**), $^+$H$_2$N−[Pro]$_x$−CO$_2$CH$_3$ (**2′**), AcN−[Pro]$_x$−CO$_2^-$ (**3**), and $^+$H$_2$N−[Pro]$_x$−CO$_2^-$ (**4**) with $x = 6$, 9, and 12 in the Gas Phase[a]

entry	N-/C-terminus	6-mer	9-mer	12-mer
1	AcN/CONH$_2$ (**1**)	0.01	−36.7	−78.5
2	AcN/CO$_2$CH$_3$ (**1′**)	−12.4	−47.8	−88.8
3	$^+$H$_2$N/CONH$_2$ (**2**)	−77.4	−119.6	−172.7
4	$^+$H$_2$N/CO$_2$CH$_3$ (**2′**)	−78.2	−124.9	−179.8
5	AcN/CO$_2^-$ (**3**)	−113.5	−169.8	−223.5
6	$^+$H$_2$N/CO$_2^-$ (**4**)	−258.4	−304.8	−346.1

[a] A negative sign denotes a preference for the PPI conformation.

electron correlation effects need to be taken into account (see the Supporting Information for details). (b) Likewise, the PPI helix becomes more and more favored when proceeding from the polyprolines with neutral end groups toward those with charged termini. Both trends are in agreement with the experimental results, as larger energy differences indicate an increased tendency to switch from the PPII into the PPI helix.

Despite the fact that the calculations were performed in the gas phase, the computed data agree well with the experimentally observed trends. However, in pure water, the PPII helix is experimentally always more stable as compared to the PPI helix regardless of the charges at the termini. This demonstrates how crucial water is for the stability of the PPII relative to the PPI helix.[13,15] To gain insight into the effect of the water on the energetic stabilities of the PPII versus the PPI helix, we considered a simple solvent model for the 6-mer. Initially, continuum models such as COSMO[36] were used that do not take direct intermolecular interactions such as hydrogen bonds between the solvent and the examined molecule into account. The COSMO model provides for the neutral 6-mer AcN−[Pro]$_6$−CO$_2$CH$_3$ an energetic preference of the PPI versus the PPII helix that is almost identical to that obtained by the calculations in the gas phase (12 kJ mol^{-1} in the gas phase versus 14 kJ mol^{-1} within the COSMO model (RI-MP2/SVP//HF/6-31G**)). This small difference in the energetics suggests that the influence of the water environment must be due to hydrogen bonding between the PPII helix and water molecules.[37]

Thus, we employed explicit water molecules in our calculations for describing solvent effects in the polyprolines. As a simple model, we used the 6-mer with seven explicit water molecules added to the carbonyl groups of the polyproline helices (details of the chosen structural model are described in the Supporting Information). The results of these calculations demonstrate a significant stabilization of the PPII versus the PPI helix by the hydrogen-bond interactions to the water molecules on the order of 60−110 kJ mol^{-1} depending on the charges of the end groups (Table 2). The PPII helix is predicted to be more stable than the PPI helix for the oligoproline with charge neutral end groups and that with a positive charge at the N-terminus (Table 2, entries 1 and 2). For the oligoproline with a negatively charged C-terminus and the zwitterionic molecule, the PPI helix is computed to be still more stable than PPII (Table 2, entries 3 and 4).

It has to be stressed that the chosen water model is an extremely crude model for the solution phase. Nevertheless, it still provides a first estimate of the expected solvent effects and their importance for the preference of the PPII helix. The data computed both with and without solvent molecules reflect the experimentally observed relative stability trends induced by the end groups, so that it seems sufficient to focus on the simple gas-phase model in the following. In future work, we plan to study solvent molecules in more detail, although it is clear that the rigorous computational description of solvent effects represents a major challenge.

Table 2. Energy Differences Computed at the RI-MP2/SVP Level in kJ mol^{-1} between the PPI and PPII ($\Delta E = E_{PPI} - E_{PPII}$) Conformation of AcN−[Pro]$_6$−CO$_2$CH$_3$, $^+$H$_2$N−[Pro]$_6$−CO$_2$CH$_3$, AcN−[Pro]$_6$−CO$_2^-$, and $^+$H$_2$N−[Pro]$_6$−CO$_2^-$ in the Gas Phase and with Seven Explicit Water Molecules[a]

entry	compound	gas phase	with H$_2$O
1	AcN−[Pro]$_6$−CO$_2$CH$_3$	−12.4	71.2
2	$^+$H$_2$N−[Pro]$_6$−CO$_2$CH$_3$	−78.2	4.3
3	AcN−[Pro]$_6$−CO$_2^-$	−113.5	−53.8
4	$^+$H$_2$N−[Pro]$_6$−CO$_2^-$	−258.4	−149.7

[a] A negative sign denotes a preference for the PPI conformation.

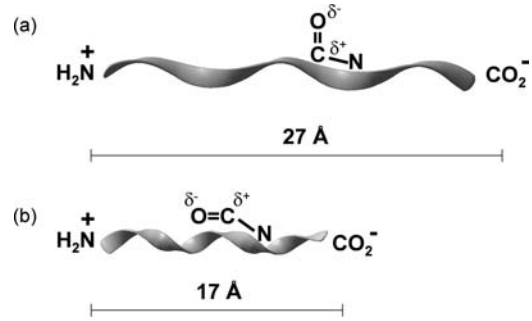

Figure 4. Schematic illustration of a 9-mer in (a) a PPII conformation and (b) a PPI conformation with the orientation of the polarized amide groups in relation to charged terminal functional groups and the distances between the termini.

Dipole Moments within the PPII and PPI Helices and Their Interaction with Charged Termini. Previous studies concerning effects of terminal functional groups on the conformation of α-helices[25] and certain helical β-peptides[26] have shown that charges at the termini induce a dipole moment along the helix axis that leads to stabilization if the charges are opposite to the polarity of the helix dipole. Whereas intramolecular hydrogen bonds are, in contrast to α-helices and β-peptides, of no importance for polyproline helices, we studied in the following the influence of dipole interactions on the conformational stability. This is expected to be most important for the polyproline helices, because the orientation of the polar amide bonds is distinctively different for the PPI and PPII conformers and will therefore affect the respective helix dipoles. Contributions from intermolecular interactions were not examined because CD spectra recorded at different concentrations are almost identical (see the Supporting Information for details).

Within the PPII conformation, the individual dipole moments of the polar amide groups are oriented almost perpendicular to the helix axis (Figures 1a and 4a). In contrast, within the PPI conformation the carbonyl groups are oriented almost parallel to the helix axis with the carbonyl oxygens pointing into the direction of the N-terminus (Figures 1b and 4b). Thus, peptides with capped termini such as **1** can be expected to have a small dipole moment in a PPII conformation and a significantly larger dipole moment in the direction from the N- to the C-terminus when adopting the PPI conformation.

(36) Klamt, A.; Schüürmann, G. *J. Chem. Soc., Perkin Trans. 2* **1993**, 799–805.
(37) (a) Sreerama, N.; Woody, R. W. *Proteins: Struct., Funct., Genet.* **1999**, *36*, 400–406. (b) Strassmair, H.; Engel, J.; Zundel, G. *Biopolymers* **1969**, *8*, 237–246.

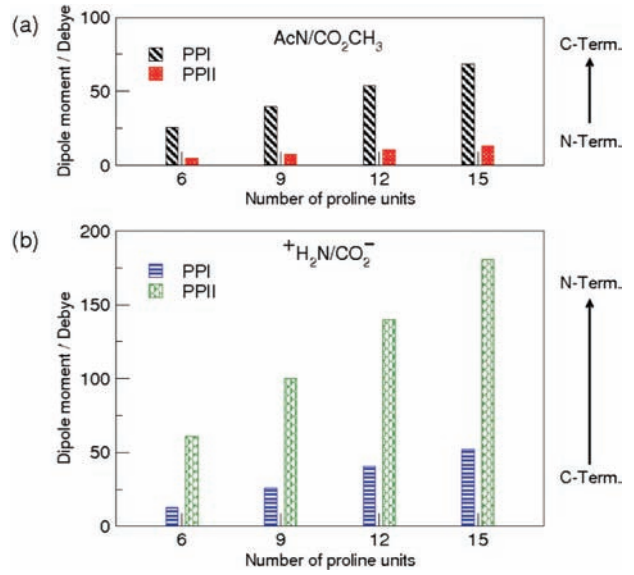

Figure 5. Dipole moments in debye calculated for (a) AcN−$[Pro]_x$−CO_2CH_3 and (b) ^+H_2N−$[Pro]_x$−CO_2^- with $x = 6$, 9, 12, and 15 for the PPI and PPII conformations at the HF/6-31G** level.

To gain a deeper understanding of the destabilization of the PPII helix relative to the PPI helix upon introduction of charged end groups, we performed additional quantum-chemical calculations at the HF/6-31G** level to compute the overall dipole moment of the different helices and the interaction of the dipole moments of the individual amide groups within the helix with the end groups. For the uncharged peptides, the calculations predict for both the PPII and the PPI helix a dipole moment approximately along the helix axis with a positive pole at the C-terminus and a negative pole at the N-terminus in significantly different strengths.[38] The dipole moment along the helix axis of the PPI helix is as expected significantly larger as compared to that of the PPII helix (Figure 5a). Roughly independently of the chain length of the oligoprolines, the dipole moments of the PPI helices are predicted to be about 5 times larger as compared to those of the PPII helices. The absolute value of the dipole moment of one proline unit amounts roughly to 4 D irrespective of whether it stems from the PPI or the PPII helix. Comparing this with the dipole moment of one turn (three units), the additivity and the impact of the orientation of the individual units become apparent: Within the PPII helix, where the polar amide bonds are perpendicular to the helix axis, the individual dipole moments almost cancel each other (2 D for one turn as compared to 4 D for one unit). In contrast, they add up to 11 D for one PPI turn due to the orientation of the amide groups roughly parallel to the molecular axis.

Upon introduction of a positive charge at the N-terminus and a negative charge at the C-terminus, the dipole moments are overcompensated by the terminal charges of the zwitterionic helices, resulting in a dipole moment with the positive pole at the N-terminus for both helices. As a result, the overall dipole moment of the PPII helices with charged termini is larger as compared to that of the respective PPI helices (Figure 5b).

The introduction of charges at the termini results for both helices in a stabilizing interaction with the individual amide dipoles. This charge−dipole interaction is considerably stronger in the more compact PPI helix due to (a) the orientation of the amide dipoles along the helix axis and (b) their closer distance toward the terminal charges. The individual interaction energies for isolated amide groups are displayed in Table 3 for the two helical forms of a 12-mer. Clearly, the charge−dipole interactions in the PPI helix are much stronger for the charged peptides (Table 3, columns B−D) as compared to the corresponding interactions in the PPII helix. In comparison, the corresponding dipole−dipole interaction energies of the neutral end groups with the amide dipoles are very small for both helical structures (Table 3, column A).

Table 3. Counterpoise Corrected Interaction Energies at the RI-MP2/SVP Level in kJ mol^{-1} between the Individual Amide Groups 2−10 (Numbered from N- to C-Terminus) and the Terminal Groups $AcNH_2/HCO_2CH_3$ (Column A), $^+H_4N/HCO_2^-$ (Column B), $^+H_4N/HCO_2CH_3$ (Column C), and $AcNH_2/HCO_2^-$ (Column D)[a]

	amide	$AcNH_2/HCO_2CH_3$, A	$^+H_4N/HCO_2^-$, B	$^+H_4N/HCO_2CH_3$, C	$AcNH/HCO_2^-$, D
PPI	2	−2.0	−25.4	−23.7	−4.9
	3	−4.7	−46.7	−41.1	−8.1
	4	−3.6	−33.3	−25.6	−8.1
	5	−1.5	−18.4	−11.7	−7.1
	6	−1.0	−15.9	−8.4	−7.8
	7	−1.2	−19.1	−7.4	−11.7
	8	−2.7	−29.3	−7.1	−23.0
	9	−3.5	−36.0	−6.9	−31.3
	10	−1.9	−39.8	−4.8	−36.3
PPII	2	−3.3	−24.2	−22.7	−3.6
	3	0.9	−3.9	−3.0	0.5
	4	−0.2	−2.7	−2.0	−0.7
	5	−0.2	−2.8	−1.9	−0.8
	6	0.2	−1.9	−0.7	−0.7
	7	−0.1	−2.4	−0.6	−1.6
	8	−0.1	−3.0	−0.6	−2.2
	9	0.4	−4.8	0.1	−4.0
	10	−2.2	−18.6	−2.5	−17.6

[a] The fragments are derived from the corresponding optimized 12-mers **1′**, **2′**, **3**, and **4**. To avoid dangling bonds, all fragments were saturated with hydrogen atoms at the cutting site. The interactions of the amide groups closest to the termini are not considered, because saturation of the fragments with hydrogen atoms would have led to artificial steric constraints. The interaction energies are critically influenced (a) by the distance of the amide dipole from the terminal charges and (b) by the orientation (angles) of the amide dipoles relative to the charges.

An additional stabilization that occurs only in the zwitterionic peptide **4** and homologues thereof stems from Coulomb interactions of the charged termini with each other. Because the distance between the charges is significantly shorter within the PPI as compared to the PPII helix, this effect favors the PPI helix over the PPII helix. The interaction energies between the terminal charges decay with the distance ($1/R$) according to Coulomb's law (Figure 6); thus, this effect is most significant for oligomers with short chain lengths. For example, the interaction energy between the termini of the more compact PPI 6-mer amounts to 161 kJ mol^{-1}, whereas in the corresponding comparatively stretched out PPII 6-mer the interaction is only 82 kJ mol^{-1} between the termini (Figure 6). Because of the distance dependence ($1/R$), this stabilization of the PPI helix becomes less and less important with longer chain lengths.

Effect of a Negatively Charged C-Terminus versus a Positively Charged N-Terminus. Experimentally as well as in the computed energy differences (see Figure 2 and Table 1), a significantly higher destabilizing effect on the PPII conformation was observed by a negatively charged carboxylate at the C-terminus

(38) Investigating electron transport in proline-rich peptides, Giese and coworkers observed a difference in the rate depending on the direction of the electron transport that corresponds to the calculated dipole moment in the PPII conformation: Giese, B.; Wang, M.; Gao, J.; Stoltz, M.; Muller, P.; Graber, M. *J. Org. Chem.* **2009**, *74*, 3621–3625.

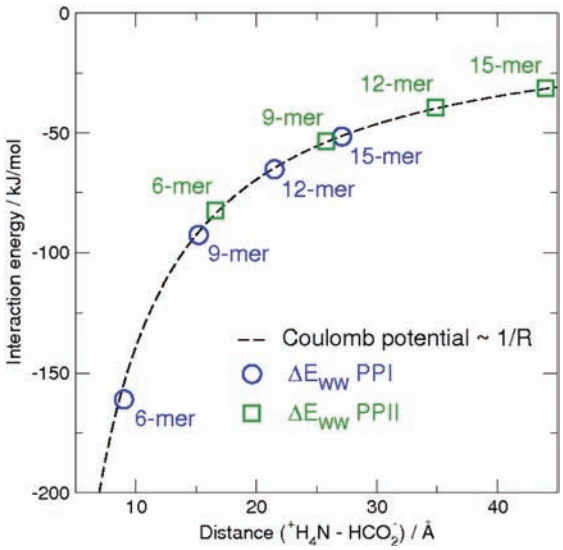

Figure 6. Counterpoise corrected interaction energies at the RI-MP2/SVP level of the two terminal groups (NH_4^+ and HCO_2^-) in the zwitterionic peptide $^+H_2N-[Pro]_n-CO_2^-$ with $n = 6$, 9, 12, and 15 plotted against the distance of the two groups in the PPI and PPII conformations.

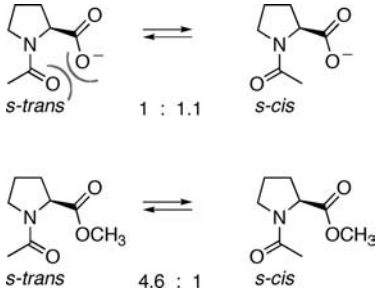

Figure 7. *s-cis*:*s-trans* conformer ratios of Ac−Pro−OH and Ac−Pro−OCH_3 at pH 7.[39]

as compared to a positively charged ammonium group at the N-terminus, despite the fact that both types of peptides have in total comparable charge−dipole interactions (Table 3, columns C and D). This effect arises from a repulsive interaction between the C-terminal carboxylate and the oxygen of the neighboring amide in a trans conformation (Figure 7). The calculations predict for the charged unit AcN−Pro−CO_2^- a favorization of the cis over the trans conformer by 22 kJ mol^{-1}, whereas the trans conformer is favored by 6 kJ mol^{-1} in the charge neutral unit AcN−Pro−CO_2CH_3 (for details, see the Supporting Information). Thus, the PPII helix consisting of trans amide bonds is favored by an uncharged C-terminus and disfavored by a negatively charged C-terminus.

These computational findings are further supported by experimental studies on acetylated proline (Ac−Pro−OH) for which a trans:cis conformer ratio of $K_{t/c} = 0.9$ in D_2O at pH 7 has been determined by ^{1}H NMR spectroscopy (Figure 7).[39] In comparison, significantly higher trans:cis conformer ratios of $K_{t/c} = 3.0$ and 4.6, respectively, are known for the protonated carboxylic acid (measured at pH 2) and the corresponding methyl ester (Ac−Pro−OCH_3).[39] Thus, the additional repulsive interaction between the carboxylate and the neighboring amide disfavors a trans amide bond at the C-terminus and therefore disfavors the PPII helix.

In contrast, neither a repulsive nor an attractive interaction occurs between a protonated amino group and the neighboring

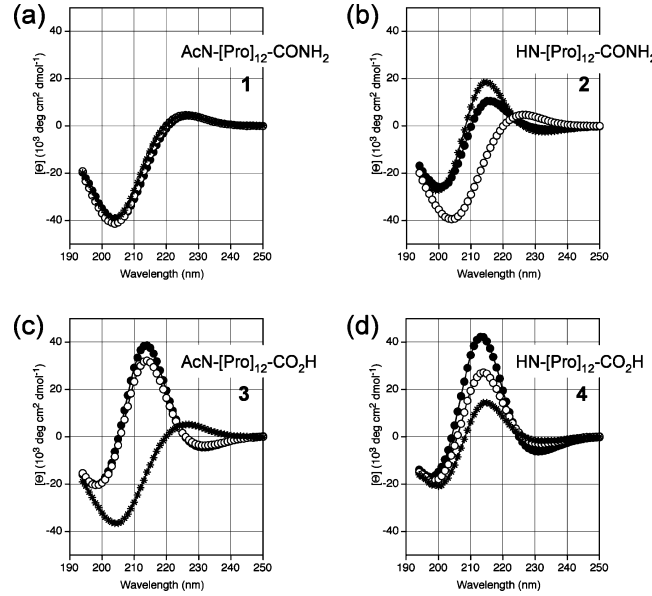

Figure 8. CD spectra of **1** (a), **2** (b), **3** (c), and **4** (d) in mixtures of 95% *n*-PrOH in aqueous phosphate buffer 10 mM, pH 7.2 (●), aqueous phosphate buffer 10 mM, pH 2.0 (*), and glycine buffer 10 mM, pH 11.7 (○). Spectra were recorded at concentrations of 50 μM (6×10^{-4} M per residue) at 25 °C.

amide.[40] This is in line with calculations of the energy difference between the N-terminal units ($^+H_2N-Pro-CONH_2$) derived from the positively charged oligoprolines (for details, see the Supporting Information).

Effect of the pH on the Conformational Stability of Peptides 1−4. The experimental and theoretical findings described so far suggest that mainly electrostatic interactions are responsible for the different equilibria between the PPII and PPI helices of peptides **1**−**4**. To further probe these conclusions, we analyzed the conformational properties of peptides **1**−**4** at different pH values. CD spectra were recorded in a mixture of 95% *n*-PrOH and 5% buffer[41] at pH 2.0, 7.2, and 11.7. Based on the findings described above, an uncharged carboxylic acid at the C-terminus and an uncharged amine at the N-terminus should favor the PPII helix as the charge−dipole interaction is lost that stabilizes the PPI helix.

As expected, the CD spectra of the capped peptide **1** without charged termini are identical regardless of the pH value of the solution and are typical of a PPII conformation (Figure 8a). In contrast, remarkable differences were observed for the other peptides at the different pH values. Peptide **2** with an amine at the N-terminus that will not bear a positive charge in basic media adopts a PPII helix in basic environment, whereas a switch to the PPI helix occurs at neutral and acidic pH (Figure 8b). Likewise, peptide **3** adopts a PPII helix in acidic environment, when the C-terminus does not bear a negative charge, whereas the PPI helix is predominant at neutral and basic pH (Figure 8c). In both cases, the CD spectra of the charge neutral peptides are very similar to those of peptide **1** with capped termini (Figure 8a−c). The spectra of peptide **4** that bears only one charge at

(39) (a) Bretscher, L. E.; Jenkins, C. L.; Taylor, K. M.; DeRider, M. L.; Raines, R. T. *J. Am. Chem. Soc.* **2001**, *123*, 777–778. (b) Hunston, R. N.; Gerothanassis, I. P.; Lauterwein, J. *J. Am. Chem. Soc.* **1985**, *107*, 2654–2661.
(40) Grathwohl, C.; Wuethrich, K. *Biopolymers* **1976**, *15*, 2043–57.
(41) The ratio of 95% *n*-PrOH in aqueous buffer was chosen because in this mixture at neutral pH all peptides with the exception of peptide **1** showed a considerable amount of PPI helicity (Figure 2).

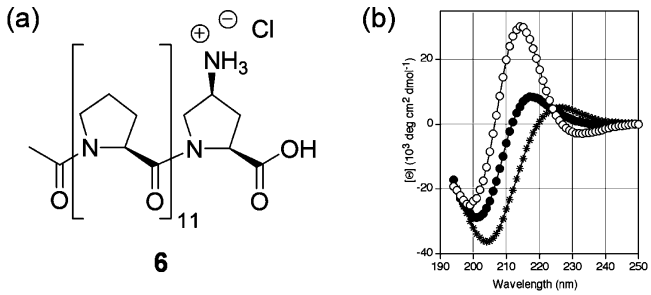

Figure 9. (a) Peptide **6** with a positive charge close to the C-terminus in acid environment. (b) CD spectra of peptide **6** in mixtures of 95% *n*-PrOH in aqueous phosphate buffer 10 mM, pH 7.2 (●), aqueous phosphate buffer 10 mM, pH 2.0 (*), and glycine buffer 10 mM, pH 11.7 (○). Spectra were recorded at concentrations of 50 μM (6×10^{-4} M per residue) at 25 °C.

basic as well as acidic pH are similar to those of peptides **2** and **3**, respectively, at pH 7.2 (Figure 8d). In addition, as observed for peptides **2** and **3**, a remaining charge at the C-terminus (at basic pH, ○) has a more pronounced destabilizing effect on the PPII helix and favors the PPI helix as compared to a charge at the N-terminus (at acidic pH, *). These results further underline that a positively charged N-terminus and a negatively charged C-terminus destabilize the PPII helix, whereas they stabilize the PPI helix.

Finally, we evaluated whether a negative charge at the C-terminus can be compensated by a neighboring positive charge. Toward this goal, peptide **6** with a (4*S*)-aminoproline [(4*S*)Amp] residue at the C-terminus was prepared and studied CD spectroscopically at different pH values (Figure 9). This peptide was also used to investigate the effect of a positive charge close to the C-terminus on the PPII/PPI equilibrium.

At neutral pH, peptide **6** bears a positively charged ammonium group close to the C-terminal end of the helix that competes with the influence of the negative charge at the C-terminal carboxylate. If the interaction with the amide-dipoles is of electrostatic nature, this should destabilize a PPI helix and favor the PPII helix as compared to Ac−Pro_{12}−OH.[42] The CD spectra of **6** in 95% *n*-PrOH and 5% buffer pH 7.2 indeed revealed a strongly reduced tendency for a PPI helix (compare Figures 8c and 9b). In an acidic environment, the C-terminal carboxylic acid is charge neutral, and the only charge remaining is the ammonium group close to the C-terminus. This disfavors a PPI conformation even more because a positive charge at the C-terminus has a stronger unfavorable interaction in the PPI helix as compared to the PPII helix. Only if the amine is not protonated (basic conditions, C-terminus deprotonated) a CD spectrum typical for a PPI helix is observed (Figure 9).

Conclusions

Our experimental and quantum-chemical results demonstrate that the conformational stability of the PPII helix is influenced by the functional groups at the C- and N-termini. Using the conformational switch of oligoprolines between the PPII and the PPI helix as a model system, we showed that the PPII helix is destabilized by a positively charged N-terminus and a negatively charged C-terminus relative to the PPI conformation, whereas capped termini have the opposite effect. This effect by charged termini is mainly due to differences in the interaction of the charged termini with the amide dipoles within the helices. These charge−dipole interactions are considerably stronger in the PPI helix as compared to the PPII helix because (a) the PPI helix is more compact and (b) the amide bonds are oriented almost linearly along the PPI helix axis with opposite polarity to the charged termini. In contrast, the amide bonds are nearly perpendicular to the axis of the PPII helix, resulting in weaker charge−dipole interactions as compared to the respective PPI helix. Our data also show that a negatively charged C-terminus has a more pronounced impact on the relative stabilities as compared to a positively charged N-terminus due to a destabilizing effect by a repulsive interaction of the carboxylate with the oxygen of the neighboring amide. Experiments at different pH values do not only support the electrostatic nature of the different conformational stabilities but also demonstrate that interconversions between the PPII and PPII structures can be triggered by changes in the pH value.

These findings are important for the development of peptides designed to have a PPII or PPI conformation. For applications of oligoprolines as molecular spacers and molecular scaffolds,[5−7] the results demonstrate that the switch between the PPII helix and the PPI helix can be facilitated or circumvented by installing the appropriate functional groups at the termini.

Experimental Section

General Aspects. Materials and reagents were of the highest commercially available grade and used without further purification. Finnigan MAT LCQ and TSQ 700 instruments were used for electrospray ionization (ESI) mass spectrometry measurements. High resolution ESI-mass spectra were measured on a Bruker FTMS 4.7T BioAPEX II instrument. Analytical HPLC was performed using a LiChrospher 100 RP-18e 5 μm (250 mm × 4 mm) column from Merck. Preparative HPLC was carried out on a LiChrospher RP-18e 5 μm (250 mm × 10 mm) column from Merck. Chirascan (Applied Biophysics Ltd., Leatherhead, UK) was used for CD measurements. For automated peptide synthesis, a Syro I Peptide Synthesizer (MultiSynTech GmbH, Witten, Germany) was employed.

General Protocols for Solid-Phase Syntheses and CD Spectroscopic Analyses. Peptides were synthesized on a 60−120 μmol scale by standard solid-phase synthesis using the Fmoc/tBu protocol. Peptides **1**, **2**, and **5** were prepared on Rink Amide resin; 2-chlorotrityl chloride resin was used for the synthesis of peptides **3**, **3a**−**c**, **4**, and **6**. 2-(6-Chloro-1*H*-benzotriazole-1-yl)-1,1,3,3-tetramethylaminium hexafluorophosphate) (HCTU)/^{i}Pr_2NEt was used for the coupling of α-*N*-Fmoc-protected amino acids to the resins.

General Procedure for Peptide Couplings on 2-Chlorotrityl Chloride Resin. Fmoc−Xxx−OH (1 equiv) and ^{i}Pr_2NEt (4 equiv) were added to a suspension of the resin in CH_2Cl_2, agitated for 1 h, and washed with a mixture of CH_2Cl_2/MeOH/^{i}Pr_2NEt (17:2:1, 3×), CH_2Cl_2 (3×), DMF (3×), and again CH_2Cl_2 (5×). The loading was determined with a quantitative Fmoc test.

General Procedure for Amino Acid Couplings. Fmoc−Xxx−OH (4 equiv), HCTU (4 equiv) dissolved in DMF, and ^{i}Pr_2NEt (16 equiv) were added to the amino-functionalized resin (~100 mM). The mixture was agitated for 1 h and washed with DMF (3×).

General Procedure for Fmoc-Deprotections. A solution of 20% piperidine in DMF was added to the resin, and the reaction mixture was agitated for 3 min, drained, and the piperidine treatment repeated for 10 min. Finally, the resin was washed with DMF (5×).

(42) In a solution of 95% *n*-PrOH in aqueous buffer that was saturated with NaCl, the PPI/PPII equilibrum of peptides **2**−**4** is shifted toward the PPII helix (see the Supporting Information) because the higher ionic strength of the NaCl solution as compared to the buffer solutions attenuates the charges at the termini. This result further supports the electrostatic nature of the observed effects (see also ref 25a).

General Procedure for Acetylation. NEt_3 (20 equiv) and Ac_2O (20 equiv) were added to the amino-functionalized resin suspended in CH_2Cl_2. The mixture was agitated for 1 h and washed with CH_2Cl_2 (7×).

General Procedure for the Cleavage of Peptides from the Solid Support. The solid supported peptides were cleaved off the resin by stirring in a mixture of acid in CH_2Cl_2 (Rink Amide resin (TFA:CH_2Cl_2 2:1) and 2-chlorotrityl chloride resin (CH_2Cl_2:AcOH:TFE 8:1:1) for 1 h and a second time for 20 min. Pooling of filtrates and removal of all volatiles under reduced pressure followed by precipitation with Et_2O afforded the peptides.

Purification. All peptides were purified by preparative HPLC on a LiChrospher RP-18e 5 μM (250 mm × 10 mm) column. Linear gradients of solvent A (CH_3CN) and solvent B (0.1% TFA in H_2O) were used. The UV-absorption was monitored at 190 nm.

General Procedure for CD Spectroscopic Analysis. CD spectra were recorded at 25 °C using a spectral bandwidth of 1 nm with a time constant of 5 s and a step resolution of 1 nm. CD data are reported as mean residual molar ellipticities (Θ_{MRW} in deg cm^2 dmol^{-1}). A quartz cell with a path length of 2 mm was used with solutions containing approximately 70 μg mL^{-1} (6×10^{-4} M per residue) peptide solutions. All samples were equilibrated for at least 12 h before measurement. CD spectra of samples measured again after a longer equilibration time of days or weeks proved identical.

Analytical Data of Peptides 1−5. Peptides **1**−**5** were prepared and purified following the general procedures.

AcN−$[Pro]_{12}$−$CONH_2$ (**1**): Analytical HPLC, t_R = 14.7 min; gradient, 93% to 66% solvent B over 20 min at a flow rate of 1 mL/min. HRMS (ESI): m/z = 1224.6783 calcd for $C_{62}H_{90}N_{13}O_{13}$ $[M + H]^+$; found, 1224.6780.

TFA·HN−$[Pro]_{12}$−$CONH_2$ (**2**): Analytical HPLC, t_R = 12.7 min; gradient, 93% to 69% solvent B over 20 min at a flow rate of 1 mL/min. HRMS (ESI): m/z = 1182.6677 calcd for $C_{60}H_{88}N_{13}O_{12}$ $[M + H]^+$; found, 1182.6652.

AcN−$[Pro]_{12}$−CO_2H (**3**): Analytical HPLC, t_R = 15.5 min; gradient, 93% to 70% solvent B over 23 min at a flow rate of 1 mL/min. HRMS (ESI): m/z = 1225.6623 calcd for $C_{62}H_{89}N_{12}O_{14}$ $[M + H]^+$; found, 1225.6609.

TFA·HN−$[Pro]_{12}$−CO_2H (**4**): Analytical HPLC, t_R = 12.3 min; gradient, 90% to 70% solvent B over 20 min at a flow rate of 1 mL/min. HRMS (ESI): m/z = 1183.6517 calcd for $C_{60}H_{87}N_{12}O_{13}$ $[M + H]^+$; found, 1183.6516.

AcN−$[Pro]_{18}$−$CONH_2$ (**5**): Analytical HPLC, t_R = 15.1 min; gradient, 90% to 70% solvent B over 21 min at a flow rate of 1 mL/min. MS (ESI): m/z (%) = 1828.9 $[M + Na]^+$, 926.5 $[M + 2Na]^{2+}$ calcd for $C_{92}H_{131}N_{19}O_{19}$.

AcN−$[Pro]_6$−CO_2H (**3a**): Analytical HPLC, t_R = 12.0 min; gradient, 93% to 70% solvent B over 22 min at a flow rate of 1 mL/min. MS (ESI, neg): m/z (%) = 642.3 $[M - H]^-$ calcd for $C_{32}H_{46}N_6O_8$.

AcN−$[Pro]_9$−CO_2H (**3b**): Analytical HPLC, t_R = 14.2 min; gradient, 93% to 70% solvent B over 22 min at a flow rate of 1 mL/min. MS (ESI, neg): m/z (%) = 932.5 $[M - H]^-$ calcd for $C_{46}H_{67}N_9O_{11}$.

AcN−$[Pro]_{18}$−CO_2H (**3c**): Analytical HPLC, t_R = 10.9 min; gradient, 88% to 65% solvent B over 16 min at a flow rate of 1 mL/min. MS (ESI, neg): m/z (%) = 1806.3 $[M - H]^-$ calcd for $C_{92}H_{120}N_{18}O_{20}$.

Synthesis and Analytical Data of AcN−[Pro]$_{11}$−[(4*S*)Amp]−CO_2H (6) (Amp = aminoproline). AcN-$[Pro]_{11}$-[(4*S*)Azp]-CO_2H (Azp = azidoproline) was synthesized according to the general procedure using Fmoc−(4*S*)Azp−OH for the first coupling onto 2-chlorotrityl chloride resin. Twelve milligrams thereof was dissolved in MeOH (1 mL), and palladium on activated carbon (5 mg, 10% Pd/C) and concentrated HCl (1 μL) were added whereupon the suspension was stirred under a hydrogen atmosphere for 7 h at room temperature. The mixture was filtered over Celite and rinsed with MeOH. The solvent was removed under reduced pressure, and the residue was precipitated with Et_2O from MeOH/CH_2Cl_2 to isolate 12 mg of **6** as a white solid. Analytical HPLC, t_R = 10.4 min; gradient, 88% to 70% solvent B over 20 min at a flow rate of 1 mL/min. MS (ESI): m/z (%) = 1263.0 (100) $[M + Na]^+$ calcd for $C_{62}H_{89}N_{13}O_{14}$.

Computational Details. The ab initio calculations have been performed using the program package TURBOMOLE[43] and a development version of the program package Q-Chem[44] employing CFMM[27] methods and the LinK[28] scheme. The basis sets 6-31G**[33] and SVP[35] were used. The contraction pattern for the SVP basis set is (4s1p)/[2s1p] for H, and (7s4p1d)/[3s2p1d] for C, N, O atoms. For SVP, only pure spherical harmonic Gaussians were employed.

Acknowledgment. This work was supported by BACHEM and the Swiss National Science Foundation. M.K. thanks Novartis for a Ph.D. fellowship, and H.W. is grateful to Bachem for an endowed professorship. S.S. thanks the "Studienstiftung des deutschen Volkes" and the Graduiertenkolleg GK441 "Chemie in Interphasen" for fellowships. C.O. acknowledges financial support from an Emmy Noether research grant of the DFG ("Deutsche Forschungsgemeinschaft") and the VolkswagenStiftung within the funding initiative "New Conceptual Approaches to Modeling and Simulation of Complex Systems".

Supporting Information Available: Additional CD spectra and details on the ab initio calculations. This material is available free of charge via the Internet at http://pubs.acs.org.

JA906466Q

(43) Ahlrichs, R.; Bär, M.; Häser, M.; Horn, H.; Kölmel, C. *Chem. Phys. Lett.* **1989**, *162*, 165–169.

(44) A development version of the program package Q-CHEM (http://www.q-chem.com/) has been used.